Original paper

Extracellular vesicles derived from human umbilical cord mesenchymal stem cells stimulate angiogenesis in myocardial infarction via the microRNA-423-5p/EFNA3 axis

Tianlin Gao, Heng Fan, Jiawen Wang, Rui Wang

Department of Cardiovascular Medicine, Ankang Central Hospital, Ankang City, China

Adv Interv Cardiol 2022; 18, 4 (70): 373–391
DOI: https://doi.org/10.5114/aic.2023.124797

Abstract

Introduction: Myocardial infarction (MI) is a severe disease that has an association with angiogenesis dysfunction.

Aim: This study explores the mechanism of extracellular vesicles (EVs) derived from human umbilical cord mesenchymal stem cells (hucMSCs) affecting angiogenesis in MI via the microRNA (miR)-423-5p/EFNA3 axis.

Material and methods: HucMSC-derived EVs (hucMSC-EVs) were isolated, extracted, and identified. EVs and human umbilical vein endothelial cells (HUVECs) were co-cultured. Migration capacity and angiogenesis ability of HUVECs were measured, and VEGF levels in cell supernatants were tested by ELISA. *In-vivo* rat MI models were established, and hucMSC-EVs were injected into the MI rat heart-infarcted area. Cardiac function, capillary density, and the degree of myocardial fibrosis were observed.

Results: HUVEC migration and angiogenesis were promoted by hucMSC-EVs, and more significantly enhanced by hucMSC-EVs containing miR-423-5p. Furthermore, miR-423-5p inhibited EFNA3 expression and EFNA3 overexpression reversed the promoting effects of EVs on HUVEC migration and angiogenesis. miR-423-5p expression was elevated and EFNA3 expression was reduced in myocardial tissues of MI rats after EV treatment. Both EVs and EVs containing miR-423-5p could improve cardiac function, reduce the area of fibrosis, and promote angiogenesis, improving cardiac repair.

Conclusions: EVs promote *in vivo* angiogenesis in MI rats via the miR-423-5p/EFNA3 axis, thus improving cardiac repair.

Key words: myocardial infarction, human umbilical cord mesenchymal stem cells, extracellular vesicles, microRNA-423-5p, EFNA3, angiogenesis.

Summary

Extracellular vesicles promote *in vivo* angiogenesis in myocardial infarction rats via the miR-423-5p/EFNA3 axis, thus improving cardiac repair.

Introduction

Myocardial infarction (MI), as a predominant cause of cardiovascular disease (CVD) mortality [1], is a devastating condition that occurs when coronary arteries are blocked and regional blood supply to the myocardium is impaired, resulting in cardiomyocyte death [2]. This disease is lethal to patients due to insufficient blood perfusion to important organs [3]. MI is a severe disease that has an association with angiogenesis dysfunction, and cell-based treatment approaches for MI with mesenchymal stem cell (MSC)-secreted exosomes have been investigated owing to their strong proangiogenic effect [4]. Therefore, it is vital to investigate the underlying molecular mechanism related to MI in treating the disease.

MSCs are able to simultaneously activate several mechanisms, and MSC transplantation is believed to be the best and most efficient method in cell therapy [5]. Human MSCs attract particular interest as a common and feasible add-on treatment for MI [2]. Human umbilical cord mesenchymal stem cells (hucMSCs) have strong self-renewal ability and multi-potency, and offer

Corresponding author:
Rui Wang, Department of Cardiovascular Medicine, Ankang Central Hospital, Ankang City 725000, China, e-mail: Wangrui40212022@163.com
Received: 22.10.2022, **accepted:** 9.12.2022.

possibilities of replacing injured cardiomyocytes [6]. Extracellular vesicles (EVs) are a heterogeneous group of membrane-limited vesicles loaded with various proteins, lipids, and nucleic acids [7]. As small membrane-bound particles produced from cells, it is indicated that EVs possess cardioprotective effects [8]. It is reported that EVs can powerfully promote angiogenesis and guard the heart against MI. In addition, EVs derived from different sources might become helpful biomarkers of cardiovascular diseases [9]. The intercellular communications between MSCs and cancer cells through MSC-EV-microRNA (miRNA) have suggested that modification of hucMSC-derived EVs (hucMSC-EVs) may be an attractive treatment selection for hucMSC-EVs' clinical application [10].

miRNA have attracted considerable attention for the capability to orchestrate changes to the transcriptome, and finally the proteome, in heart failure [11]. Evidence has shown that miR-423-5p possesses a cardiac origin [12], and miR-423-5p is associated with congestive heart failure [13]. Moreover, miR-423-5p might act as valuable biomarkers in patients with left ventricular (LV) heart failure or patients with LV remodeling after MI [14]. EphrinA3 (EFNA3) is one member of the ephrin protein family that elicits short-distance cell-cell signaling, and it promotes or represses tumorigenesis depending on tumor types [15]. Specifically, EFNA3 is implicated in vascular remodeling and apoptosis in the heart [16]. Besnier *et al.* found that in endothelial cells, miR-210 represses EFNA3, inducing proangiogenic responses [17].

Aim

Taking the active functions of EVs, miR-423-5p, and EFNA3 into consideration, we performed this study to discover the essential role of hucMSC-EVs' delivery of miR-423-5p in MI by targeting EFNA3.

Material and methods

Ethics statement

The use of all animals was ratified by the Experimental Ethics Committee of our hospital.

Cell culture

HucMSCs and human umbilical vein endothelial cells (HUVECs), procured from Wuhan Procell Life Science & Technology Co., Ltd. (Wuhan, China), were incubated in Dulbecco's modified Eagle's medium (DMEM, Gibco, USA) supplemented with 10% fetal bovine serum (FBS, Gibco), 100 U/ml penicillin, and 100 µg/ml streptomycin at 37°C in a humidified atmosphere containing 5% CO_2. These cells were passaged every 3 days, and the hucMSCs at passages 3-7 were utilized for subsequent experiments [18].

HucMSC identification

Multiplex differentiation ability: HucMSCs were incubated in OriCell hucMSC osteogenic and adipogenic differentiation medium (Cyagen Biosciences Inc., Guangzhou, China), respectively, and stained using oil red O solution and alizarin red solution, respectively, to evaluate the accumulation of intracellular lipid droplets and calcium deposits [19, 20].

EV isolation and identification

EVs were extracted *in vitro* from the hucMSC medium. Before utilization, FBS in the medium was ultracentrifuged at 100,000 g for 12 h to remove EVs from the serum. The cells were inoculated in 6-well plates at 2 × 10^5 cells/well, and continued to incubate with an EV-free serum for 48 h for the harvest of the cell supernatants. Subsequently, hucMSC-derived EVs (hucMSC-EVs) were isolated by differential centrifugation. All the centrifugation steps were done at 4°C, while the other steps were conducted on ice. The specific steps were as follows: centrifugation at 500 g for 15 min, 2000 g for 15 min, and 10,000 g for 20 min to remove dead cells and debris. A 0.22 µM filter was utilized to remove smaller cell debris and then ultracentrifuged at 100,000 g for 70 min, followed by resuspension in phosphate-buffered saline (PBS) for a second ultracentrifugation under the same conditions. The precipitate was stored at –80°C for further or immediate use.

EV identification with transmission electron microscopy (TEM): 20 µl of EVs was supplemented dropwise on the copper grid, left for 3 min, and then supplemented dropwise with 30 µl of phosphotungstic acid solution (pH 6.8) after aspirating the liquid from the side with filter paper, re-stained for 5 min at room temperature, then dried with incandescent light, and photographed under the TEM.

EV surface markers were identified by western blot: EV suspensions were concentrated and their protein content was determined by a BCA kit (Thermo Fisher Scientific, MA, USA). Sodium dodecyl sulfate-polyacrylamide gel electrophoresis (SDS-PAGE) gels were prepared, and then protein denaturation and electrophoresis were performed. After that, membranes were transferred and assayed for EV-specific marker proteins Hsp70 (ab5442), CD81 (ab79559), Alix (ab117600), and Calnexin (ab112995) (all from Abcam, UK) [21, 22].

Uptake of hucMSC-EVs by HUVECs

EVs were marked with the PKH26 Red Fluorescent Kit (Sigma Aldrich, USA). Specifically, EVs collected after 100,000 g ultracentrifugation were cultured with PKH26 dye previously diluted in diluent C solution at room temperature for 10 min. The labeled EVs were rinsed by PBS ultracentrifugation. PKH26-labeled EVs were suspended in a low-serum medium and cultured with HUVECs for 12 h. Cell nuclei were stained with 4′-6-diamidi-

no-2-phenylindole (DAPI) and analyzed by fluorescence microscopy.

Lentiviral and plasmid packaging, and cell transfection

For lentiviral infection, hucMSCs during the logarithmic growth phase were digested with trypsin, counted, and then inoculated in 6-well plates with DMEM diluted for transfection. The lentiviral plasmid encoding miR-423-5p and its corresponding negative control (miR-NC) were designed and produced by Genechem (Shanghai, China). HucMSCs were transfected with the lentivirus at a multiplicity of infection (MOI) of 20. These cells were screened with 1 µg/ml of puromycin for 3 days.

HucMSC grouping and treatment: cultured hucMSCs were separated into the PBS group, EV group (extraction of hucMSC-EVs), EV-miR-NC group (extraction of hucMSC-EVs containing the lentiviral plasmid miR-NC), and EV-miR-423-5p group (extraction of hucMSC-EVs containing the lentiviral plasmid miR-423-5p).

HUVECs were transiently transfected. pcDNA-3.1 EFNA3, miR-423-5p mimic, and the corresponding NCs were obtained from Genechem. HUVECs were cultured in 6-well plates at an inoculation density of 4×10^5 cells/ml. When cell fusion reached 80%, the cells were transfected following Lipofectamine 2000 instructions (Invitrogen, New York, California, USA). Next, the cells were transfected with 250 µl of serum-free Opti-MEM (Gibco) to dilute miRNA mimic or plasmid in each group and evenly mixed with 10 µl of Lipofectamine 2000 for 5 min, and supplemented dropwise to the cell culture wells after standing for 20 min. After transfection, the cells of different groups were incubated at 37°C under 5% CO_2 for 48 h for subsequent related experiments.

Co-culture experiments

HUVECs were inoculated in 6-well plates, and after reaching 70-80% confluence, they were incubated with PBS and EVs, respectively, for 24 h, and then incubated with hypoxia and serum deprivation (h/SD) for 12 h for subsequent experiments. The researchers had no knowledge of the group assignments during the experiments [18].

HUVECs angiogenesis test

The capillary tube formation assay was utilized to assess HUVECs' angiogenesis. HUVECs (30,000 cells/well) were inoculated into 96-well plates covered with growth factor-reduced Matrigel. Capillary-like tube formation was photographed 6 h later. Image J software (National Institutes of Health, NIH) was utilized to quantify tube length.

Transwell assay

In vitro cell migration assays were conducted in 24-well plates using a Transwell chamber (pore size: 8 mm, Corning, USA). A Transwell chamber without Matrigel was prepared, and the lower chamber was prefilled with 600 ml of 20% FBS medium and equilibrated at 37°C for 1 h. HUVECs were resuspended in an FBS-free medium, and 1×10^6 cells were inoculated into the upper chamber and incubated at 37°C and 5% CO_2 for 24 h. After that, the Transwell chamber was fixed with 5% glutaraldehyde at 4°C, and dyed with 0.1% crystal violet for 5 min. The surface cells were wiped off with cotton balls, observed under an inverted fluorescence microscope (TE2000, Nikon, China), and photographed from 5 randomly selected fields. The number of cells through the chamber per group was regarded as the average value. Differences between groups were analyzed and histograms of migration were plotted.

Enzyme-linked immunosorbent assay (ELISA)

VEGF concentration in serum and cell supernatants was tested with an ELISA kit (MSKBIO, Wuhan, China). The absorbance (A) values of each well at 450 nm were tested within 3 min using a full-range microplate reader (Synergy 2, BioTek, USA). To calculate the regression equation of the standard curve, the standard concentration was utilized as the horizontal coordinate and the A value as the vertical coordinate, and the sample A value was substituted into the equation to calculate the concentration of the target protein in the sample [23].

Luciferase assay

Bioinformatics software (http://www.targetscan.org) predicted the targeting relationship between miR-423-5p and EFNA3 and the binding site of miR-423-5p to the EFNA3 3'UTR. The 3'-UTR sequence of EFNA3 containing the presumed miR-423-5p binding sites (WT) or mutated binding sites (MUT) were inserted into the pGL3 (Promega, WI, USA) plasmid, thereby constructing the EFNA3-WT and EFNA3-MUT plasmids. Logarithmically grown HUVECs were inoculated in 96-well plates and then transfected with Lipofectamine 2000 (Invitrogen). EFNA3-WT and EFNA3-MUT, together with miR-423-5p mimic and its NC, were transfected into HUVECs with 3 replicates per group. After 48 h, the Dual-Luciferase Reporter Assay System kit (Promega, USA) was implemented to detect luciferase activity [24].

Reverse transcription-quantitative polymerase chain reaction (RT-qPCR)

RNA was extracted by the TRIzol method (Invitrogen). miRNA was reversely transcribed utilizing the MiRcute miRNA First-strand cDNA synthesis kit (Tiangen Biotech, Beijing, China) and mRNA was reverse-transcribed implementing the PrimeScript RT reagent Kit (Promega, Madison, WI, USA). After that, SYBR Green PCR Master Mix (Life Technologies, Carlsbad, CA, USA) was used to quantify gene expression. The relative transcript levels of the

Table I. Primer sequences for RT-qPCR

Gene	Forward (5–3′)	Reverse (5–3′)
miR-423-5p	TGAGGGGCAGAGAGCGAGACTTT	Universal reverse primer
U6	TGCGGGTGCTCGCTTCGGCAGC	Universal reverse primer
hsa-EFNA3	TGTACTGGAACAGCTCCAAC	AGATAGTCGTTCACGTTCACCT
rno-EFNA3	ATGAATTCCATGCCGGCCAA	AAGTCTTTGGAGGCGCAGCA
hsa-GAPDH	CTGGGCTACACTGAGCACC	AAGTGGTCGTTGAGGGCAATG
rno-GAPDH	CTCTCTGCTCCTCCCTGTTC	TCACACCGACCTTCACCATC

miR-423-5p – microRNA-423-5p, EFNA3 – ephrinA3, GAPDH – glyceraldehyde-3-phosphate dehydrogenase.

target genes were determined using the relative quantification method ($2^{-\Delta\Delta CT}$ method). Glyceraldehyde-3-phosphate dehydrogenase (GAPDH) was considered as the internal reference gene for mRNA and U6 was considered as the internal reference for miRNA. All reactions were repeated 3 times. The primer sequences are detailed in Table I.

MI animal model establishment

Male Sprague Dawley rats (6–8 weeks old) were housed in standard rat cages with ventilation, quietness, and natural light. The room temperature was maintained at 23–25°C; the relative humidity was kept at 55–60%. The rats were fed and watered freely, and the bedding in the cages was changed daily by a dedicated person.

The rats were anesthetized intraperitoneally with pentobarbital sodium (50 mg/kg) and then connected to a ventilator via oral tracheal intubation. After fixation, a left-sided thoracotomy was conducted between the 3rd and 4th intercostal space under aseptic conditions, and the anterior descending branch of the left coronary artery was ligated 1.5 mm below the inferior border of the left auricle. After the MI model was successfully established, MI rats were randomly grouped into 4 groups (n = 10): 1) MI group: the MI model was established; 2) MI + EV group: after successful establishment of the MI model, EVs (50 µg) were injected at the border of the infarct area; 3): MI + EV-miR-NC group: after successful establishment of the MI model, EV-miR-NC (50 µg) was injected at the border of the infarct area; 4): MI + EV-miR-423-5p group: after successful establishment of the MI model, EV-miR-423-5p (50 µg) was injected at the border of the infarct area. The sham group was regarded as the control group (n = 10). Carprofen (10 mg/kg) was utilized for postoperative analgesia to ensure that the animals did not suffer additional pain. All those who performed surgery and subsequent analyses were blinded to the intervention [18, 25].

Cardiac function evaluation

Cardiac function was assessed by transthoracic echocardiography (VEVO 2100, VisualSonics, USA) after 2 weeks of EV treatment. The rats were anesthetized by intraperitoneal injection of pentobarbital sodium (50 mg/kg) and put on a heated platform in the supine position. The LV internal diameter was determined by a 30 MHz transducer from a short-axis view recorded in m-mode. Left ventricular ejection fraction (LVEF) and left ventricular shortening fraction (LVFS) were recorded by implementing Vevo analysis software to evaluate cardiac function.

Masson staining

To detect fibrosis, heart tissue sections embedded in paraffin were stained with Masson staining [26]. The infarct area was measured as the average ratio of fibrotic area to total ventricular area. The sections were observed and photographed under a microscope, and analyzed by Image J software.

Immunohistochemistry

Paraffin sections of heart tissues were heated at 60°C for 1 h, dewaxed and hydrated in xylene I and xylene II, dehydrated in gradient alcohol, soaked in 3% hydrogen peroxide at room temperature for 20 min to eliminate endogenous peroxidase activity, and blocked with 10% goat serum for 15 min. Primary antibodies CD31 (ab28364, 1 : 50, Abcam, USA) and VEGF (19003-1-AP, 1 : 200, Proteintech, Rosemont, IL, USA) were added to the sections and cultured overnight at 4°C, then biotin-labeled goat anti-rabbit IgG (ab6721, Abcam) secondary antibody working solution was added dropwise and cultured for 40 min at room temperature. After that, the sections were developed by DAB for 10 min, re-stained with hematoxylin for 1 min, dried in gradient alcohol dehydration, cleared by xylene, and blocked utilizing neutral gum. PBS was used as an NC instead of a primary antibody. The final results were double-blindly scored by two persons [27].

Statistical analysis

The experiment was repeated at least 3 times. SPSS 21.0 software and GraphPad Prism 8.0 software were implemented for assessing statistical differences. The data were expressed as mean ± standard deviation. Comparison of data between two groups was performed by the unpaired t-test, and one-way analysis of variance (ANOVA) was implemented for comparison among multiple groups, with Tukey's post hoc test. $^*P < 0.05$ was considered to indicate statistical significance.

Results

hucMSC-EVs are enriched with miR-423-5p

To investigate the role of EVs secreted by hucMSCs, we first identified hucMSCs. Under light microscopy, hucMSCs were long spindle-shaped or spindle-shaped, growing in colonies, and the cells were arranged in a swirling pattern when densely packed (Figure 1 A). Meanwhile, hucMSCs were subjected to adipogenic and osteogenic differentiation assays, and it was found that hucMSCs had good adipogenic and osteogenic differentiation (Figure 1 B). EVs were further isolated from hucMSCs. TEM analysis revealed that EVs isolated from hucMSC supernatant were cup-shaped (Figure 1 C). Western blot results (Figure 1 D) showed that the hucMSC-EVs expressed characteristic proteins such as CD81, Alix, and Hsp70, while they negatively expressed calnexin. These results indicated that we successfully isolated hucMSC-EVs. We found miR-423-5p presented in MSCs by the EVmiRNA Database (Figure 1 E), and we further examined the content of miR-423-5p in hucMSC-EVs using RT-qPCR, and found that miR-423-5p could be enriched in hucMSC-EVs (Figure 1 F).

The above findings suggested that hucMSC-EVs were enriched with miR-423-5p, and miR-423-5p was delivered to HUVECs.

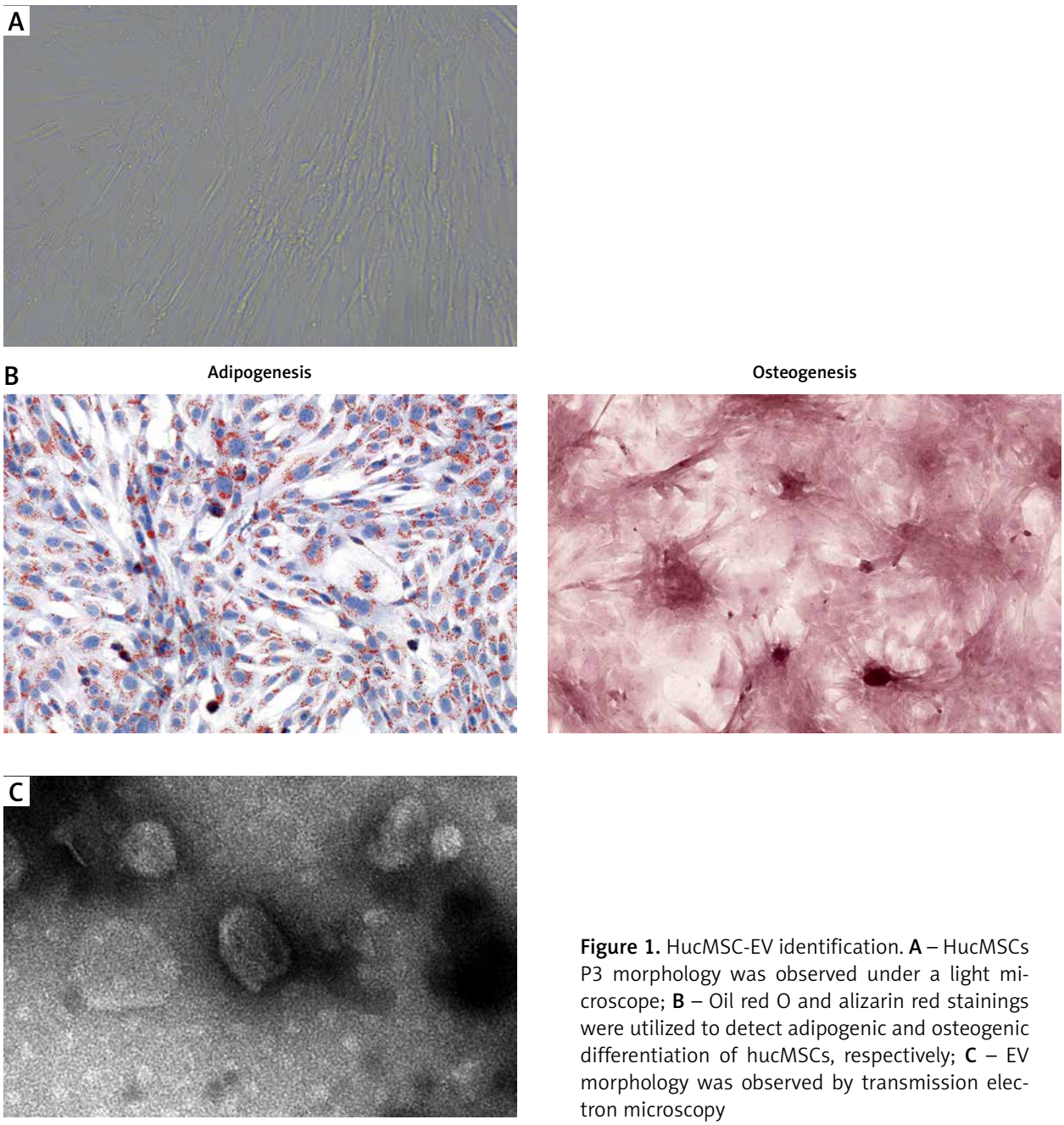

Figure 1. HucMSC-EV identification. **A** – HucMSCs P3 morphology was observed under a light microscope; **B** – Oil red O and alizarin red stainings were utilized to detect adipogenic and osteogenic differentiation of hucMSCs, respectively; **C** – EV morphology was observed by transmission electron microscopy

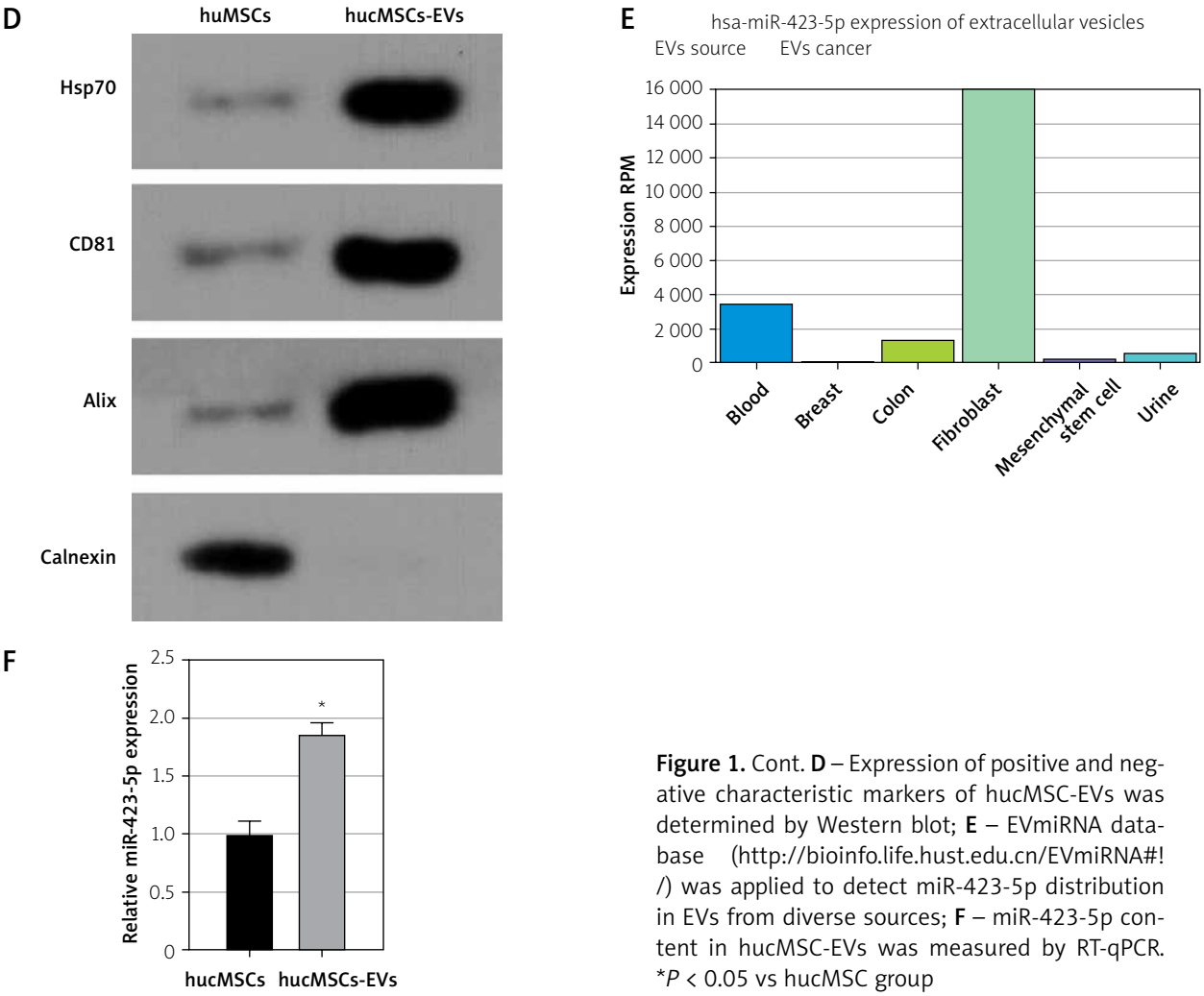

Figure 1. Cont. **D** – Expression of positive and negative characteristic markers of hucMSC-EVs was determined by Western blot; **E** – EVmiRNA database (http://bioinfo.life.hust.edu.cn/EVmiRNA#!/) was applied to detect miR-423-5p distribution in EVs from diverse sources; **F** – miR-423-5p content in hucMSC-EVs was measured by RT-qPCR. **P* < 0.05 vs hucMSC group

hucMSC-EVs promote *in vitro* tube formation of HUVECs by delivering miR-423-5p

To further explore whether hucMSC-EVs could enter into HUVECs, we co-incubated PKH26-labelled EVs with HUVECs. Fluorescence microscopy (Figure 2 A) revealed that PKH26-labelled hucMSC-EVs were gradually internalized by HUVECs. miR-423-5p expression in hucMSCs and hucMSC-EVs was further tested by RT-qPCR, and the experimental results demonstrated that miR-423-5p expression was increased in both hucMSCs and EVs infected with miR-423-5p (Figure 2 B). The above results indicated that HUVECs could take up hucMSC-EVs, thereby increasing miR-423-5p expression levels in HUVECs.

To determine whether miR-423-5p transferred *in vitro* could effectively regulate HUVECs' angiogenic capacity, we overexpressed miR-423-5p in hucMSCs, then isolated EVs and co-cultured EVs with HUVECs, and the results indicated that miR-423-5p expression was elevated in HUVECs after co-culture with EVs or EV-miR-NC, and miR-423-5p expression was higher in HUVECs co-cultured with EV-miR-423-5p (Figure 2 C). The migration and angiogenic abilities of HUVECs after co-culture with hucMSC-EVs were further examined, and the results revealed that HUVECs' migration and angiogenic ability and VEGF levels were raised upon treatment with EVs, while the increase in migration and angiogenic capacity of HUVECs, as well as VEGF levels, upon treatment with EV-miR-423-5p was more significant (Figures 2 D–F).

The above experimental results demonstrated that hucMSC-EVs could promote *in vitro* tube formation by delivering miR-423-5p to HUVECs.

miR-423-5p inhibits EFNA3

Previous studies have demonstrated that EFNA3 has a significant association with angiogenesis and that EFNA3 downregulation promotes angiogenesis [17, 28]. The bioinformatics website TargetScan predicted that miR-423-5p and EFNA3 had specific binding regions and were highly conserved in multiple species (Figures 3 A, B). Luciferase assay was further conducted to verify that EFNA3 was a target of miR-423-5p. EFNA3-WT luciferase activity was reduced in hucMSCs transfected with miR-423-5p mimic, while luciferase activity of EFNA3-MUT showed no significant difference (Figure 3 C). Meanwhile,

RT-qPCR was conducted to test EFNA3 expression in HUVECs, and the experimental results revealed that miR-423-5p expression was raised in hucMSCs transfected with miR-423-5p mimic, while the expression of EFNA3 was reduced (Figure 3 D). This indicated that miR-423-5p was specifically bound to the EFNA3 gene.

miR-423-5p regulates EFNA3 to affect *in vitro* tube formation of HUVECs

To further investigate whether hucMSC-EVs delivered miR-423-5p to affect *in vitro* tube formation of HUVECs by regulating EFNA3, we transfected pcDNA-EFNA3 into HUVECs and extracted hucMSC-EVs to treat HUVECs. The results of RT-qPCR revealed that EFNA3 expression levels were increased in HUVECs transfected with pcDNA-EFNA3. Furthermore, pcDNA-EFNA3 transfection could reverse the inhibiting effects of hucMSC-EVs on EFNA3 expression in HUVECs (Figure 4 A). Subsequently, the findings of pseudo-tube formation and Transwell assays demonstrated that pseudo-tube formation and migration capabilities of HUVECs were diminished in hucMSCs transfected with pcDNA-EFNA3, and pcDNA-EFNA3 re-

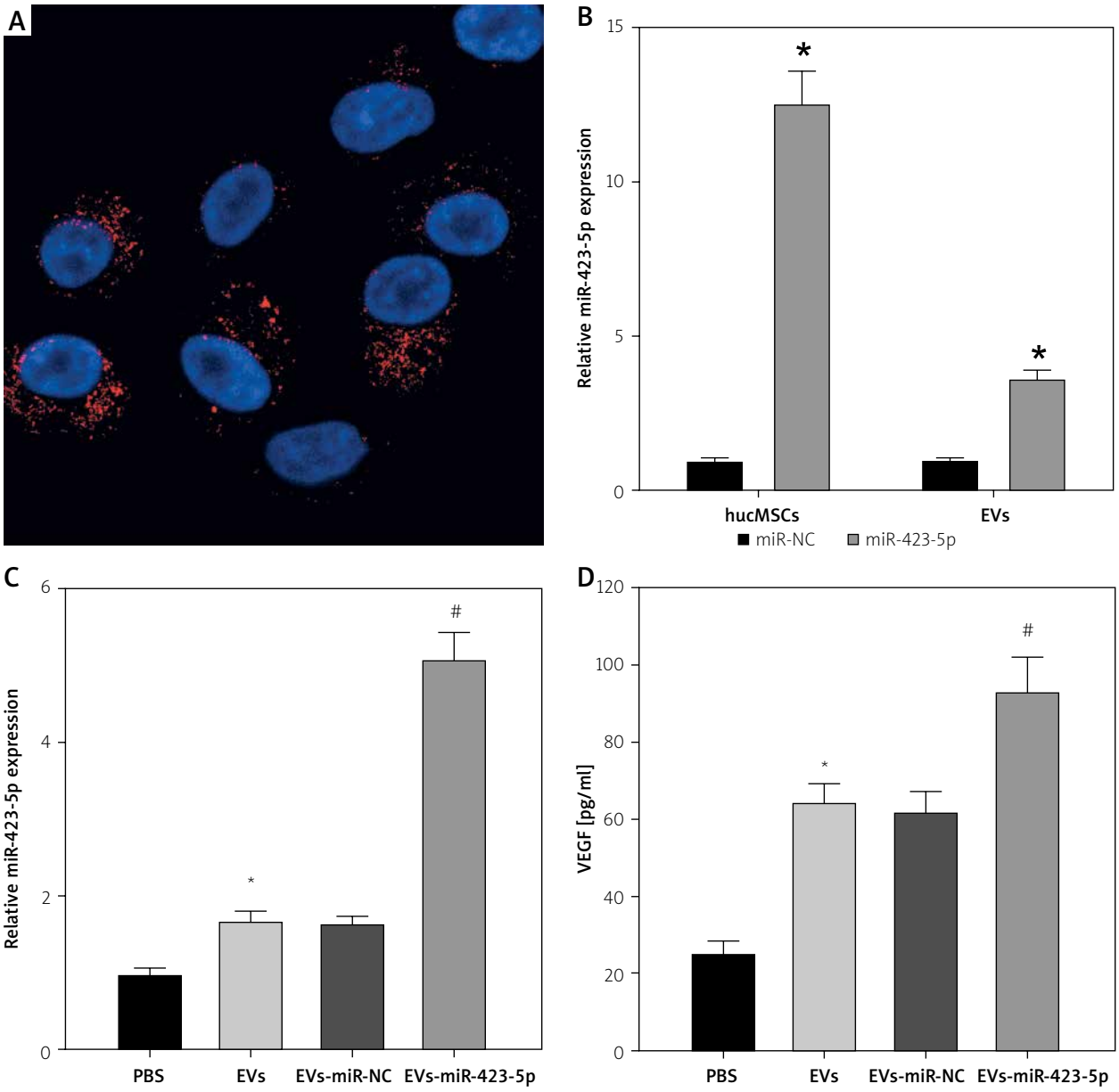

Figure 2. HucMSC-EVs promote *in vitro* tube formation of HUVECs by delivering miR-423-5p. **A** – HUVECs were cultured with PKH26-labelled EVs (red) and endocytosis of EVs was detected by immunofluorescence assay; **B** – miR-423-5p expression in hucMSCs and EVs was tested by RT-qPCR; **C** – miR-423-5p expression in HUVECs was measured by RT-qPCR; **D** – VEGF content in cell supernatants was measured by ELISA. **P* < 0.05 vs. PBS group or miR-NC group, #*p* < 0.05 vs. EV-miR-NC group

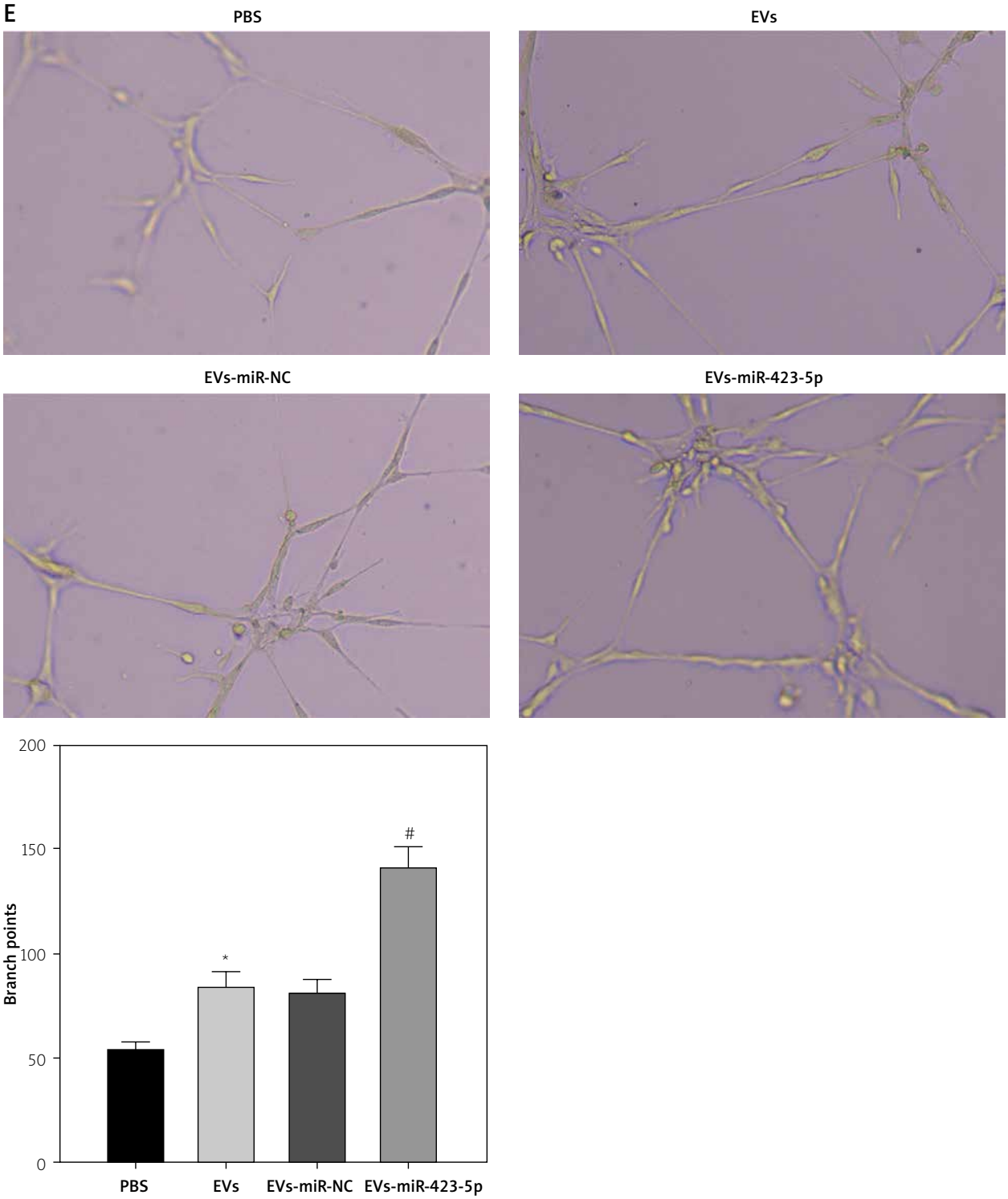

Figure 2. Cont. **E** – Angiogenic ability of HUVECs in each group was evaluated by pseudo-tube formation assay. **P* < 0.05 vs. PBS group or miR-NC group, #*p* < 0.05 vs. EV-miR-NC group

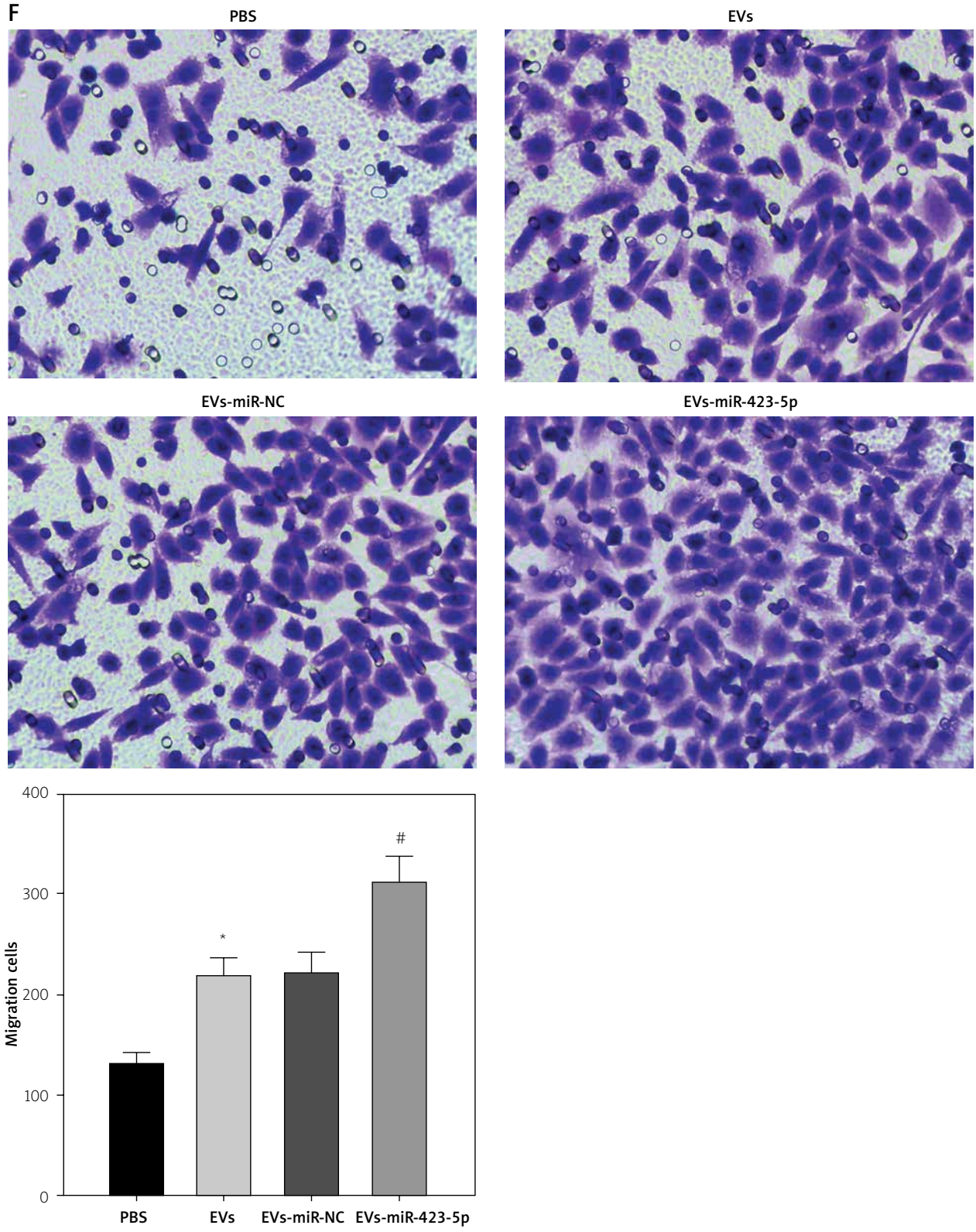

Figure 2. Cont. **F** – Migration ability of HUVECs in each group was detected by Transwell assay. **P* < 0.05 vs. PBS group or miR-NC group, #*p* < 0.05 vs. EV-miR-NC group

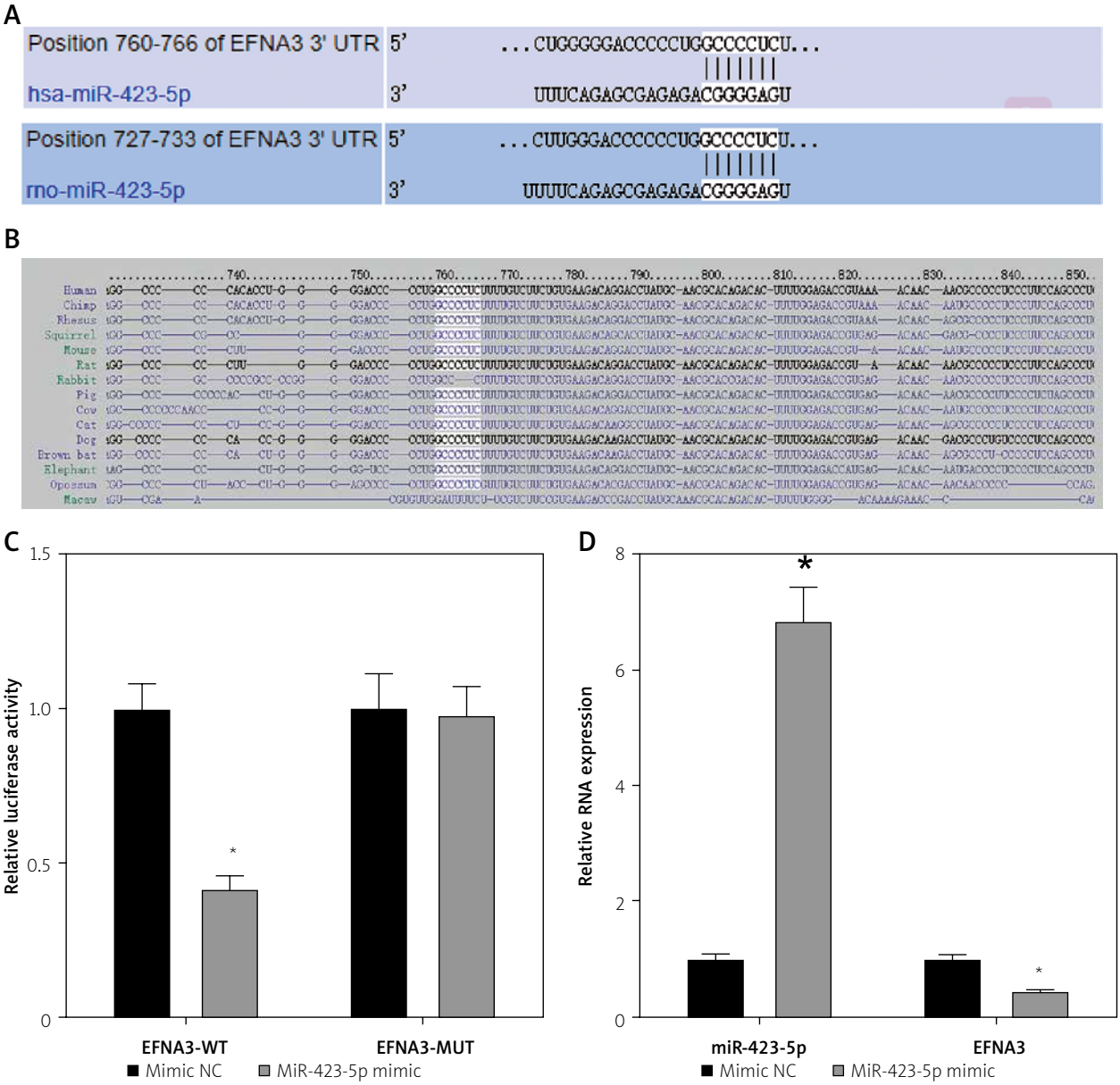

Figure 3. Targeting relationship between miR-423-5p and EFNA3. **A** – Bioinformatics website TargetScan (https://www.targetscan.org/) predicted there were binding sites between EFNA3 and miR-423-5p; **B** – Binding sites between miR-423-5p and EFNA3; **C** – Results of dual luciferase reporter gene assay; **D** – miR-423-5p and EFNA3 mRNA expression levels in HUVECs were tested by RT-qPCR. *$P < 0.05$ vs. mimic NC group

versed the promoting effects of hucMSC-EVs on HUVECs pseudo-tube formation and migration (Figures 4 B–D). The above results indicated that hucMSC-EV-miR-423-5p can promote HUVECs' pseudo-tube formation and migration by inhibiting EFNA3.

EVs effectively protect cardiac function of MI rats *in vivo* by delivering miR-423-5p

To evaluate *in vivo* EVs' effects on rat cardiac function, EVs were injected into MI rats. miR-423-5p and EFNA3 expression in myocardial tissues was tested by RT-qPCR, and the results showed that miR-423-5p expression was decreased while EFNA3 expression was increased in MI rats, and in the MI rats injected with EVs, miR-423-5p expression was elevated and EFNA3 expression was reduced. In addition, the trend was more pronounced in MI rats injected with EV-miR-423-5p (Figure 5 A). Furthermore, the cardiac function of rats in each group was evaluated, and it was found that there was a decrease in cardiac function as well as LVEF and LVFS values in MI rats, and there was a significant improvement in cardiac impairment and an increase in LVEF and LVFS values in MI rats injected with EVs, with a more pronounced trend in MI rats injected with EVs -miR-423-5p (Figure 5 B).

To further explore *in vivo* hucMSC-EV miR-423-5p therapeutic potential in fibrosis and angiogenesis, Masson staining was conducted and the results showed a reduction in the area of fibrosis in MI rats injected with EVs (Figure 5 C). Capillaries were stained using immunohistochemistry with anti-CD31 and VEGF. After 2-week EV treatment of myocardial infarction, capillary density in the peri-infarct area was increased in MI rats injected with EVs (Figures 5 D, E). Additionally, this trend was more pronounced in MI rats injected with EV-miR-423-5p (Figures 5 D, E). EVs reduced the fibrosis area and promoted angiogenesis, thus significantly benefiting cardiac repair.

These results indicated that miR-423-5p secreted by hucMSC-EVs had a potential protective effect on cardiac function in infarcted rats.

Discussion

MI is a cardiovascular disorder with high mortality, and hucMSCs with forceful self-renewal capacity and multipotency offer the possibility of replacing damaged cardiomyocytes [6]. Advances have been achieved to identify the pathology and inhibit progression of the disease. Considering the delivery role of hucMSC-EVs, we revealed that hucMSC-EVs' delivery of miR-423-5p alleviated MI in rats by suppressing EFNA3.

EVs are diverse, nanoscale membrane vesicles that are actively produced by cells [29]. As particles secreted by diverse cells, EVs are often observed to mimic their parent cell properties; as such, those originating from developmental sources hold promise in the treatment of a vast range of diseases including MI [30]. EVs originating from different cell types have potential to transport complicated information to endothelial cells and to induce pro- or antiangiogenic signaling [31]. In our study, we found that EVs reduced the fibrosis area and promoted angiogenesis, thus significantly benefiting cardiac repair. Similarly, in acute myocardial infarction (AMI), injured cardiac muscle cells release EVs with elevated levels of angiogenic, anti-apoptotic, mitogenic, and growth factors for the purpose of inducing infarcted myocardium repair and healing [32]. Meanwhile, MSC-EVs significantly improve cardiac function and angiogenesis in the post-MI heart. MSC-EVs increase the tube formation ability and proliferative and migratory ability of HUVECs [33].

miRNAs can modulate transcripts in situ and act as paracrine mediators in influencing angiogenesis at distant sites. miRNAs can shift cardiac proliferation, differentiation, maturation, as well as pathological remodeling responses to injury, stress, along with abnormal regulator expression [34]. Exosomal miRNAs are implicated in regulating endothelial cell function and angiogenesis [35]. It is supported that miR-423-5p has a relation to the prognosis of acute decompensated heart failure [36]. Early in acute MI, miR-423-5p expression in plasma is raised following normalization within 6 h, suggesting that miR-423-5p is a possible early marker of myocardial necrosis [37]. In our work, we evaluated the role of hucMSC-EVs, and finally noted that miR-423-5p could be enriched in hucMSC-EVs. Next, we evaluated the effects of miR-423-5p delivered by hucMSC-EVs in HUVECs, and eventually proved that hucMSC-EVs could promote *in vitro* tube formation by delivering miR-423-5p to HUVECs. Actually, it was previously demonstrated that the

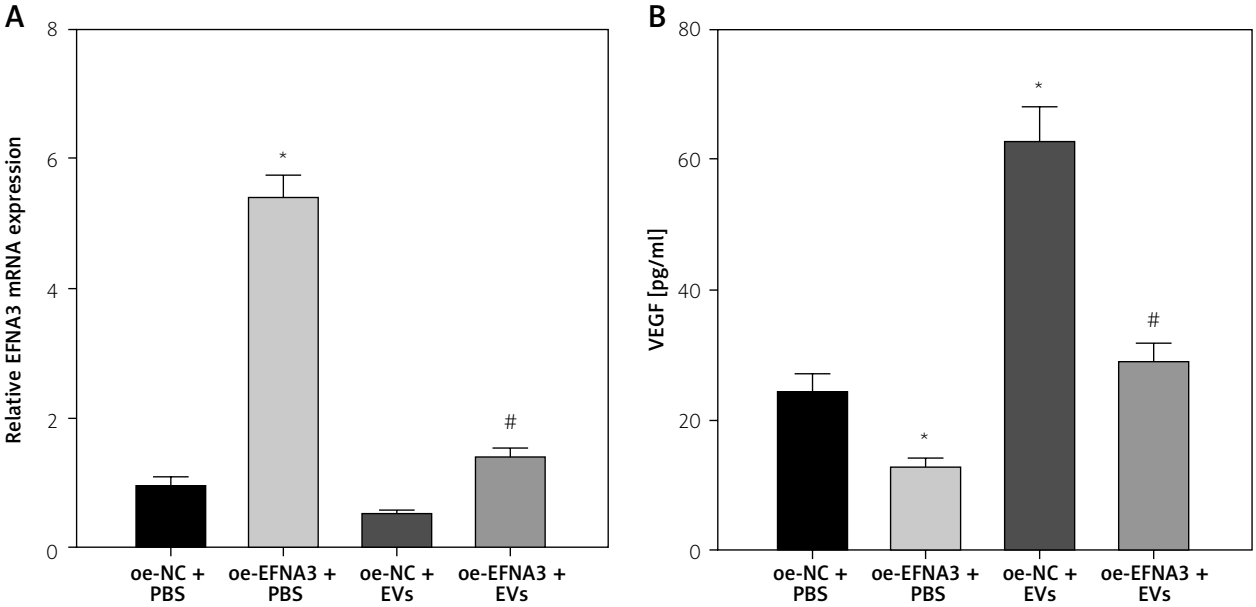

Figure 4. Interaction effect of miR-423-5p and EFNA3 on *in vitro* tube formation of HUVECs. **A** – EFNA3 mRNA expression levels in HUVECs were assessed by RT-qPCR; **B** – HUVEC migration ability of each group was measured by Transwell assay. **P* < 0.05 vs. the oe-NC + PBS group, #*p* < 0.05 vs. the oe-NC + EV group

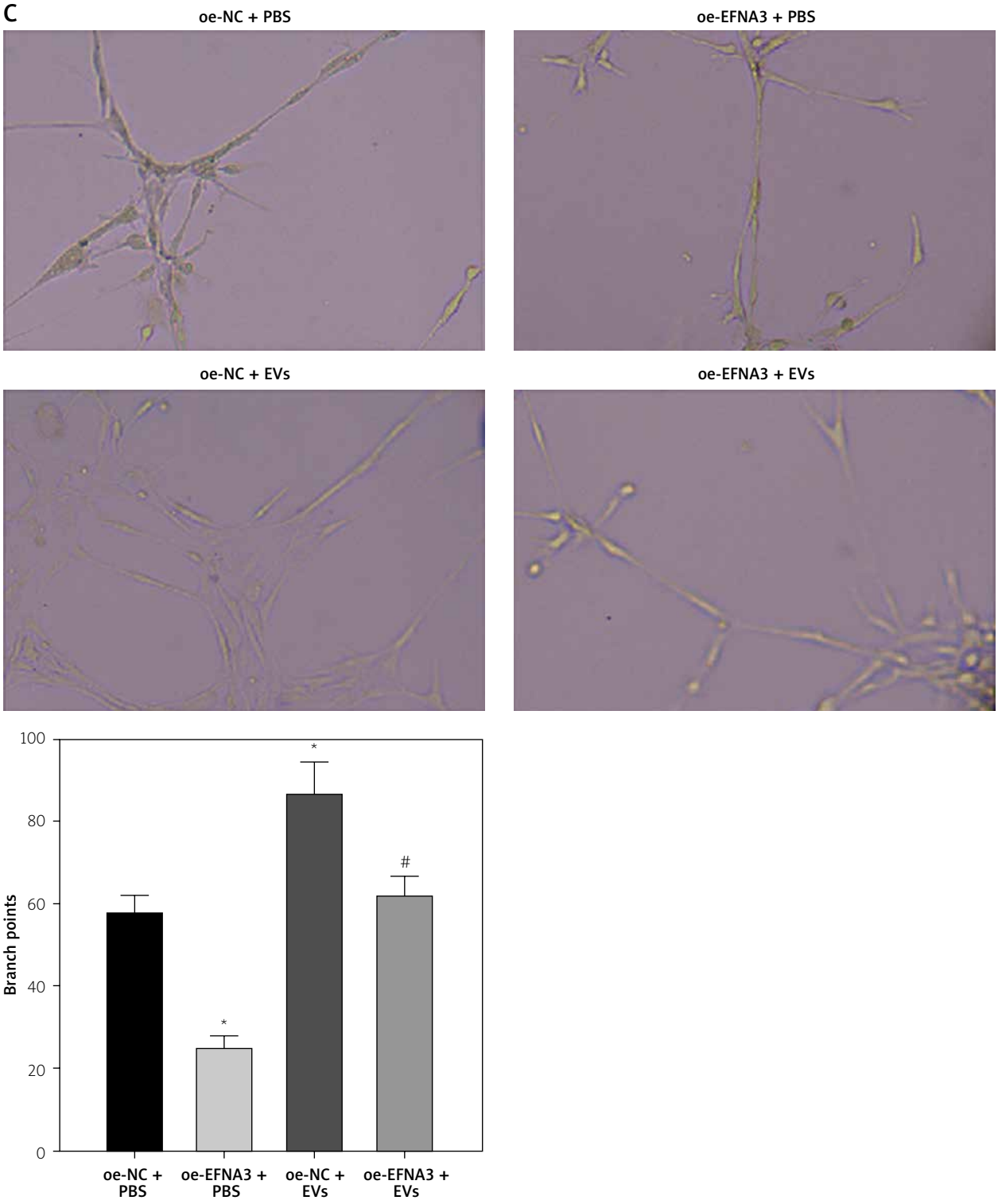

Figure 4. Cont. **C** – HUVEC angiogenic ability of each group was evaluated by pseudo-tube formation assay. *$P < 0.05$ vs. the oe-NC + PBS group, #$p < 0.05$ vs. the oe-NC + EV group

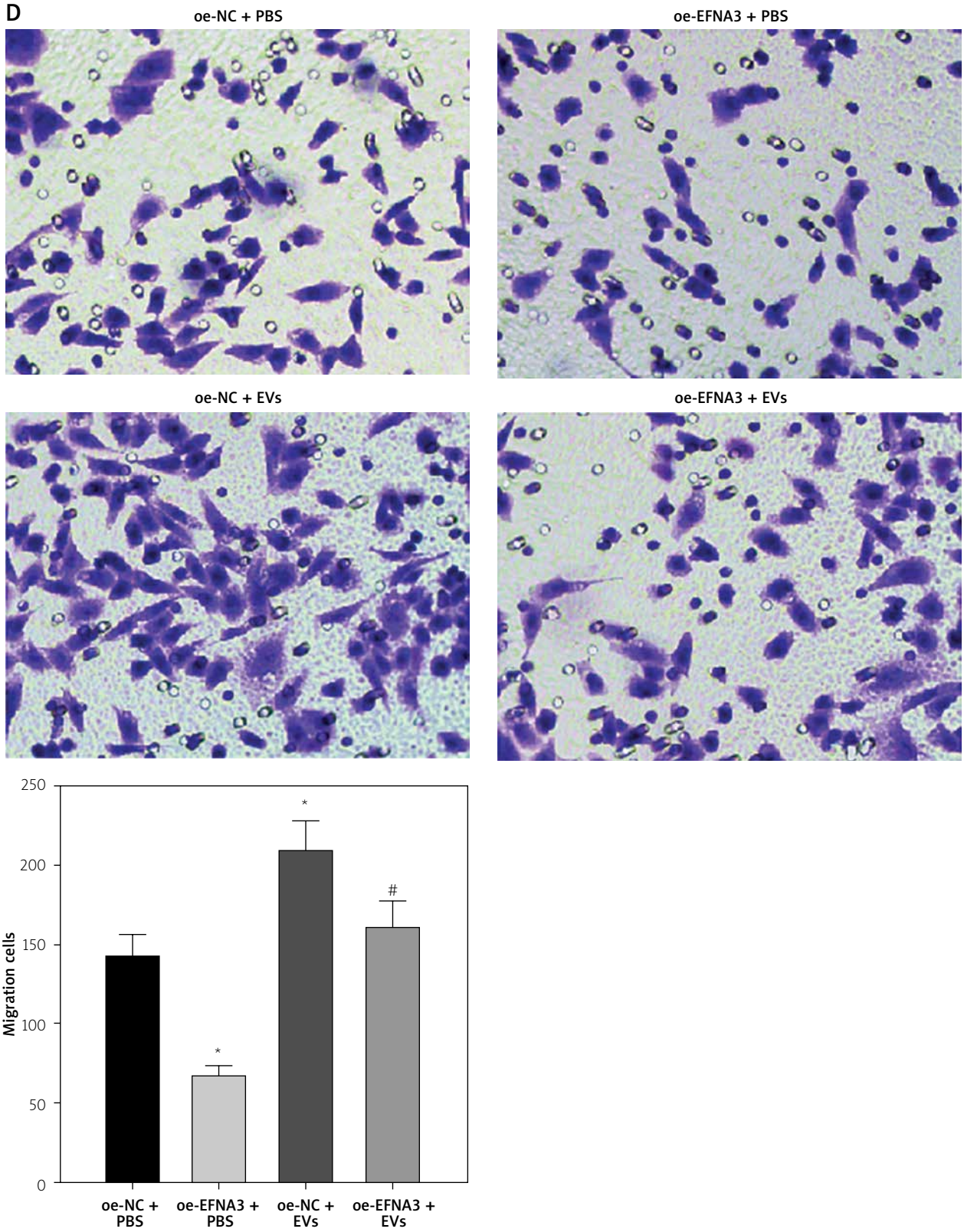

Figure 4. Cont. **D** – VEGF content in cell supernatants was tested by ELISA. **P* < 0.05 vs. the oe-NC + PBS group, #*p* < 0.05 vs. the oe-NC + EV group

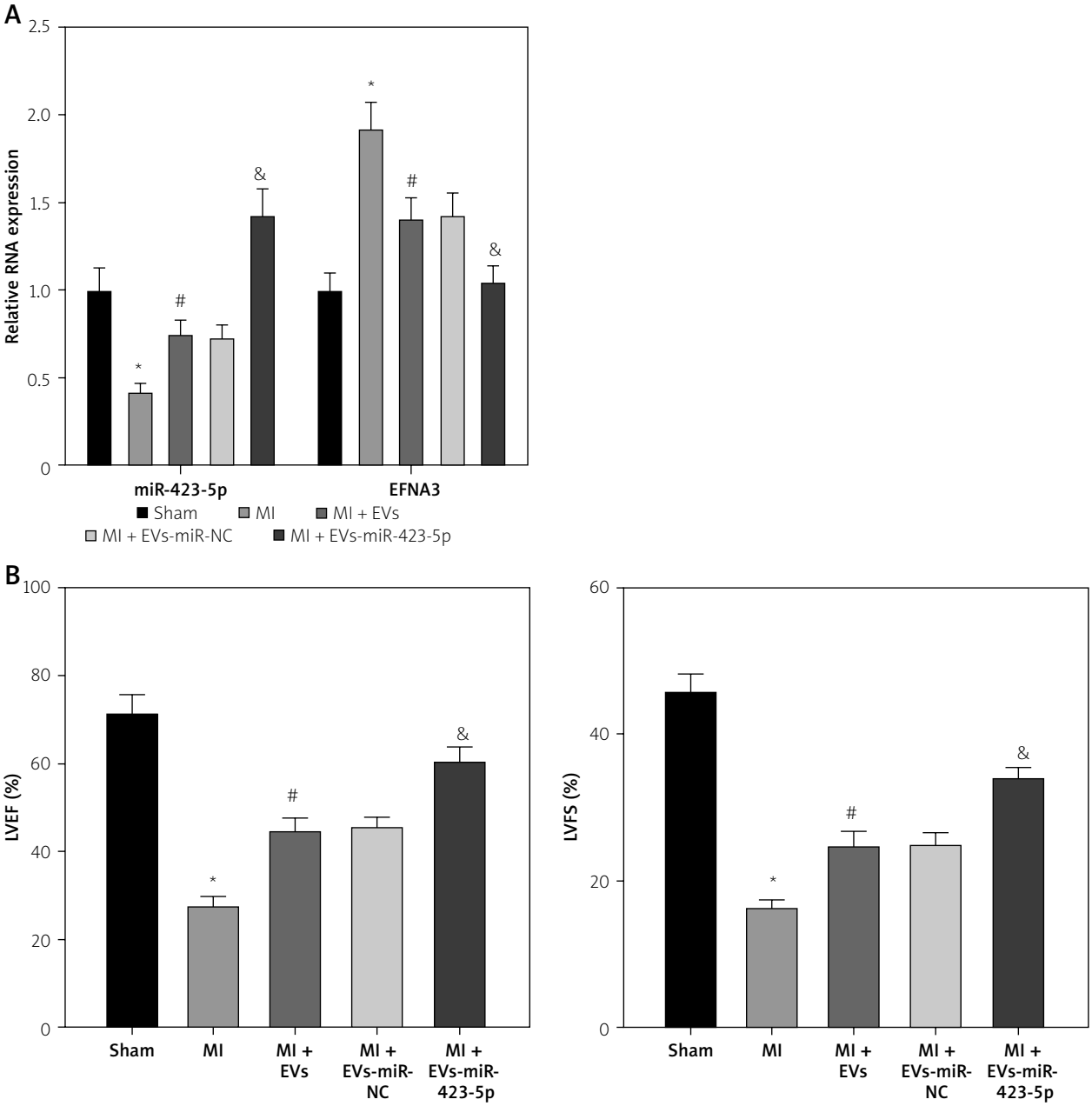

Figure 5. *In vivo* experiments for observing the effects of EV-miR-423-5p on cardiac function repair in MI rats. **A** – miR-423-5p in myocardial tissues was measured by RT-qPCR; **B** – LVEF and LVFS were determined by echocardiography to assess cardiac function. **P* < 0.05 vs the sham group, #*p* < 0.05 vs. the MI group, &*p* < 0.05 vs. the MI + EV-miR-NC group

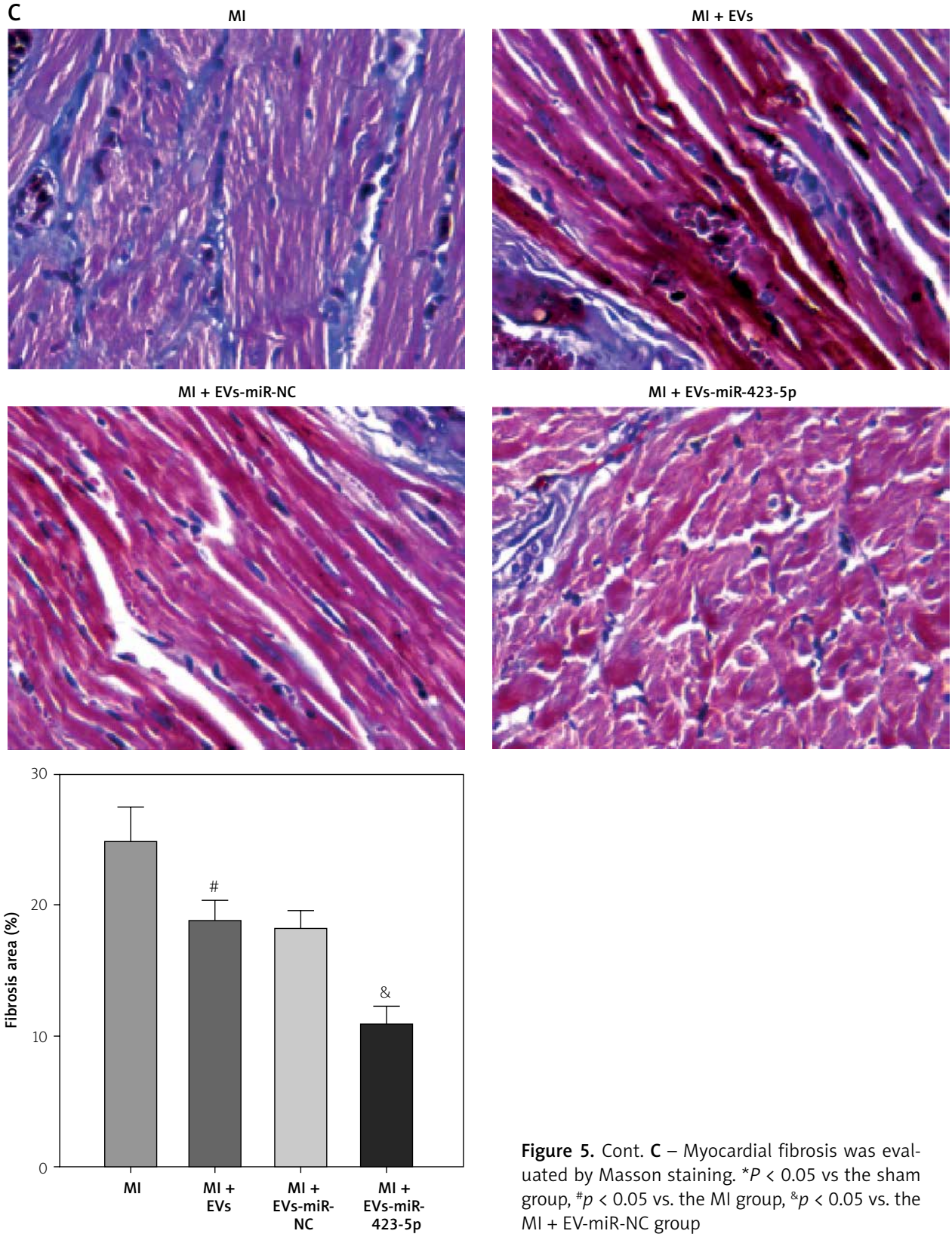

Figure 5. Cont. **C** – Myocardial fibrosis was evaluated by Masson staining. *$P < 0.05$ vs the sham group, #$p < 0.05$ vs. the MI group, &$p < 0.05$ vs. the MI + EV-miR-NC group

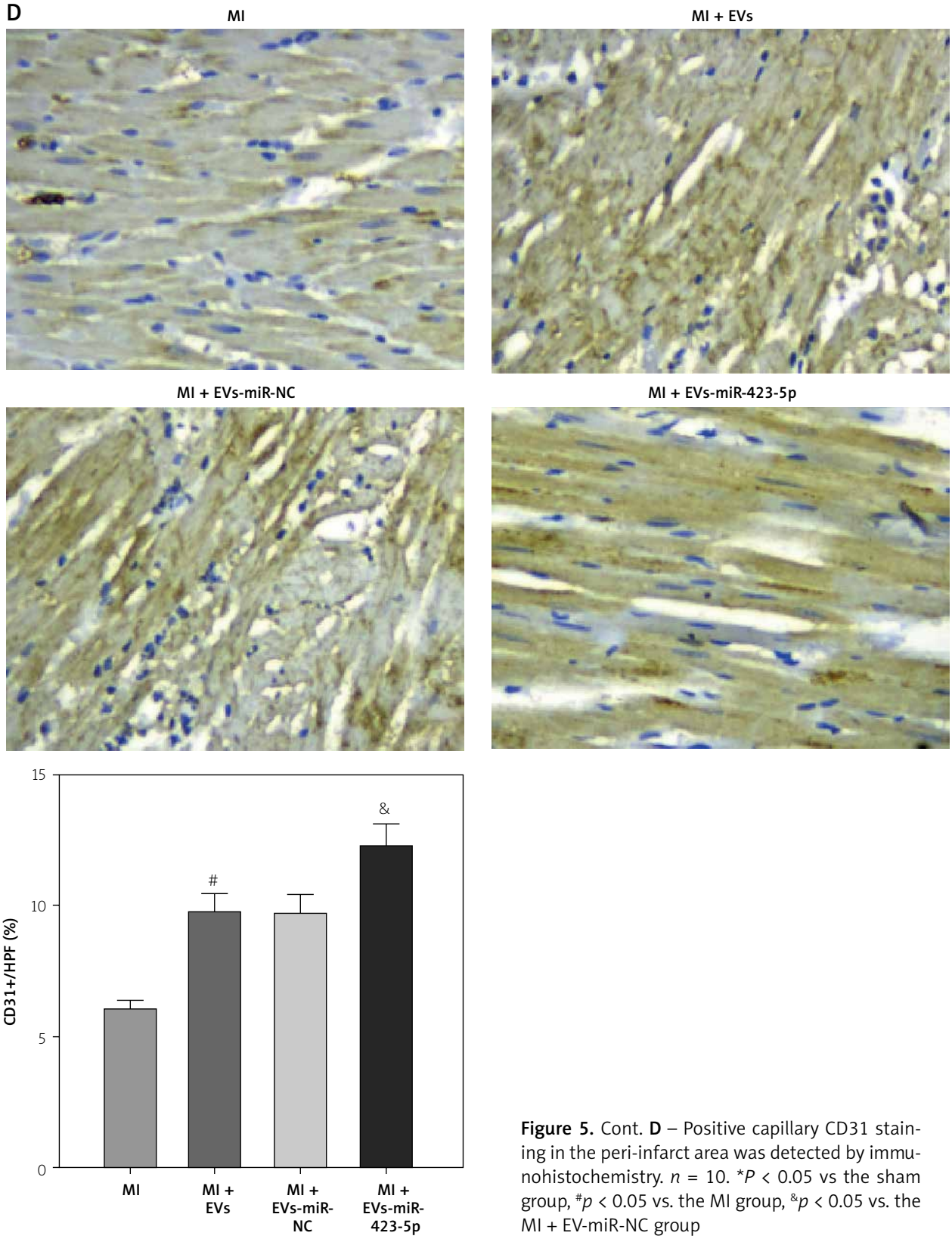

Figure 5. Cont. **D** – Positive capillary CD31 staining in the peri-infarct area was detected by immunohistochemistry. $n = 10$. $^{*}P < 0.05$ vs the sham group, $^{\#}p < 0.05$ vs. the MI group, $^{\&}p < 0.05$ vs. the MI + EV-miR-NC group

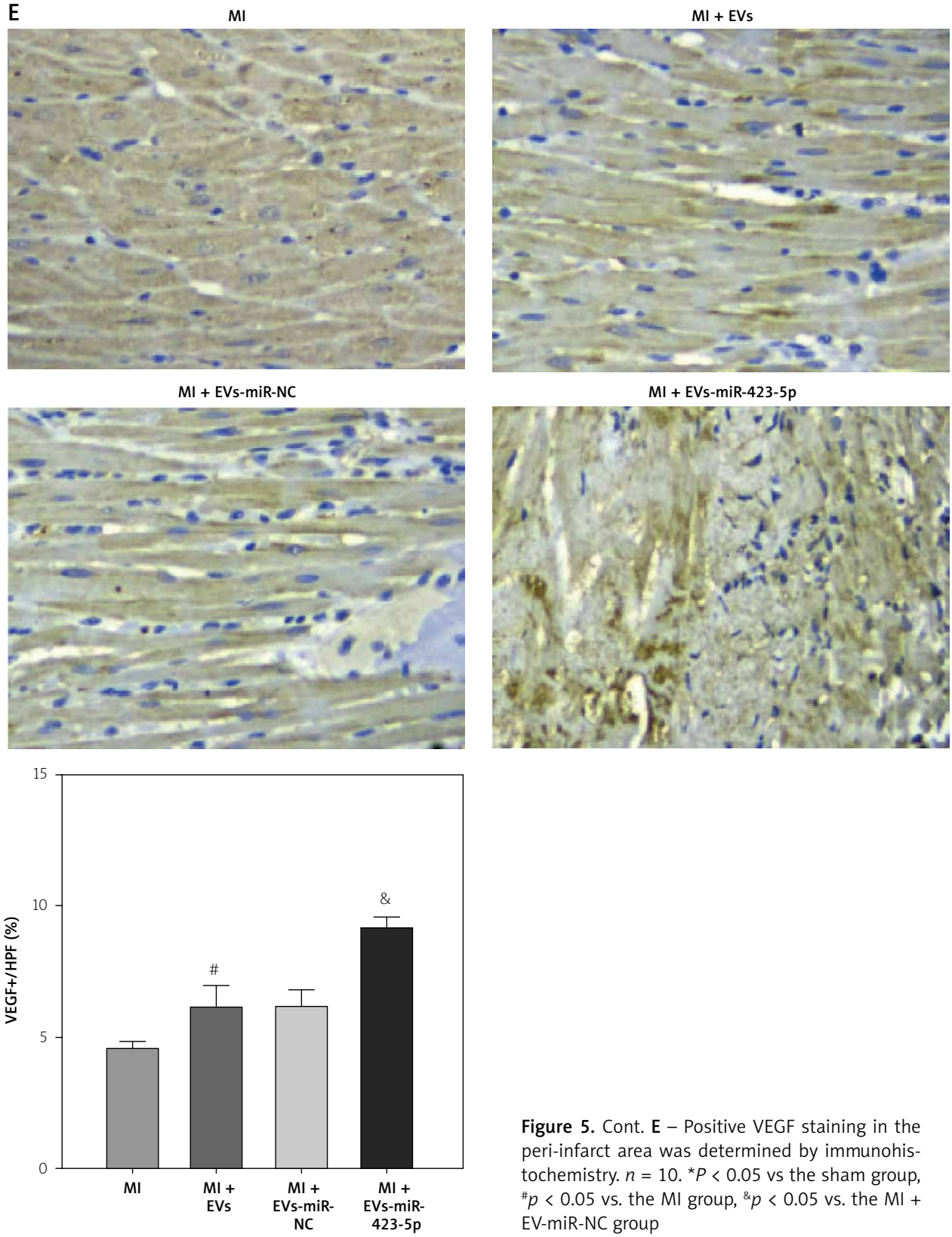

Figure 5. Cont. **E** – Positive VEGF staining in the peri-infarct area was determined by immunohistochemistry. $n = 10$. $^{*}P < 0.05$ vs the sham group, $^{\#}p < 0.05$ vs. the MI group, $^{\&}p < 0.05$ vs. the MI + EV-miR-NC group

increase of miRNA sequences in the HepG2-secreted EVs indicates high levels of miR-423-5p [38]. There are articles focusing on the interactions of EVs with other miRNAs in MI. For instance, it was reported that delivery of miR-486-5p-engineered EVs safely promotes angiogenesis and heart function in a nonhuman primate MI model and may benefit cardiac repair [39]. Furthermore, in our study, *in-vivo* rat MI models were established, and hucMSC-EVs were injected into the MI rat heart infarcted area. Cardiac function, capillary density, and the degree of myocardial fibrosis were observed. The corresponding findings demonstrated that miR-423-5p secreted by hucMSC-EVs had a potential protective effect on cardiac function in infarcted rats.

The downstream gene involved in the functions of miR-432-5p secreted by hucMSC-EVs in MI was further analyzed. Previous studies have revealed that EFNA3 is linked to angiogenesis and EFNA3 downregulation promotes angiogenesis [17, 28]. At last, we validated the control of EFNA3 by miR-423-5p in MI. It was found that miR-423-5p was specifically bound to the EFNA3 gene, and was further demonstrated that hucMSC-EV-miR-423-5p could stimulate HUVECs' pseudo-tube formation and migration by inhibiting EFNA3. MSC-EVs are sufficient to evoke angiogenesis and exert therapeutic effects on MI, and their pro-angiogenesis influence could be related to a miR-210- EFNA3 dependent mechanism [33]. Furthermore, small EVs derived from hypoxic MSCs evoke vascularized bone regeneration via the miR-210-3p/EFNA3/PI3K pathway [28].

To briefly conclude, our study showed that miR-423-5p delivered by hucMSC-EVs improves the cardiac function of MI rats and angiogenesis of HUVECs. Our study has deepened the understanding of the miR-423-5p/EFNA3 axis-modulated MI progression, and provided a basis for advancing potential therapeutics in MI. Our research is based on animal trials in the absence of clinical data, which is the major limitation of our analysis. Therefore, further research should be focused on clinical samples to validate the findings of our research. Additionally, in the *in vitro* experiments, we used only HUVEC as a model to investigate MI-induced angiogenesis. However, the mechanisms affecting MI are multifaceted, such as inflammatory response, oxidative stress, and apoptosis, which require further exploration in the follow-up work.

Conflict of interest

The authors declare no conflict of interest.

References

1. Piamsiri C, Maneechote C, Siri-Angkul N, et al. Targeting necroptosis as therapeutic potential in chronic myocardial infarction. J Biomed Sci 2021; 28: 25.
2. Laundos TL, Vasques-Novoa F, Gomes RN, et al. Consistent long-term therapeutic efficacy of human umbilical cord matrix-derived mesenchymal stromal cells after myocardial infarction despite individual differences and transient engraftment. Front Cell Dev Biol 2021; 9: 624601.
3. Shi HT, Huang ZH, Xu TZ, et al. New diagnostic and therapeutic strategies for myocardial infarction via nanomaterials. EBioMedicine 2022; 78: 103968.
4. Sun J, Shen H, Shao L, et al. HIF-1alpha overexpression in mesenchymal stem cell-derived exosomes mediates cardioprotection in myocardial infarction by enhanced angiogenesis. Stem Cell Res Ther 2020; 11: 373.
5. Shareghi-Oskoue O, Aghebati-Maleki L, Yousefi M. Transplantation of human umbilical cord mesenchymal stem cells to treat premature ovarian failure. Stem Cell Res Ther 2021; 12: 454.
6. Sun Y, Liu J, Xu Z, et al. Matrix stiffness regulates myocardial differentiation of human umbilical cord mesenchymal stem cells. Aging 2020; 13: 2231-50.
7. Abels ER, Breakefield XO. Introduction to extracellular vesicles: biogenesis, RNA cargo selection, content, release, and uptake. Cell Mol Neurobiol 2016; 36: 301-12.
8. Yadid M, Lind JU, Ardona HAM, et al. Endothelial extracellular vesicles contain protective proteins and rescue ischemia-reperfusion injury in a human heart-on-chip. Sci Transl Med 2020; 12: eaax8005.
9. Sluijter JPG, Davidson SM, Boulanger CM, et al. Extracellular vesicles in diagnostics and therapy of the ischaemic heart: Position Paper from the Working Group on Cellular Biology of the Heart of the European Society of Cardiology. Cardiovasc Res 2018; 114: 19-34.
10. Dong L, Pu Y, Zhang L, et al., Human umbilical cord mesenchymal stem cell-derived extracellular vesicles promote lung adenocarcinoma growth by transferring miR-410. Cell Death Dis 2018; 9: 218.
11. Pinti MV, Hathaway QA, Hollander JM. Role of microRNA in metabolic shift during heart failure. Am J Physiol Heart Circ Physiol 2017; 312: H33-45.
12. Goldraich LA, Martinelli NC, Matte U, et al. Transcoronary gradient of plasma microRNA 423-5p in heart failure: evidence of altered myocardial expression. Biomarkers 2014; 19: 135-41.
13. Luo P, He T, Jiang R, Li G. MicroRNA-423-5p targets O-GlcNAc transferase to induce apoptosis in cardiomyocytes. Mol Med Rep 2015; 12: 1163-8.
14. Bauters C, Kumarswamy R, Holzmann A, et al. Circulating miR-133a and miR-423-5p fail as biomarkers for left ventricular remodeling after myocardial infarction. Int J Cardiol 2013; 168: 1837-40.
15. Yiminniyaze R, Zhang X, Zhu N, et al. EphrinA3 is a key regulator of malignant behaviors and a potential prognostic factor in lung adenocarcinoma. Cancer Med 2023; 12: 1630-42.
16. Hu S, Huang M, Li Z, et al. MicroRNA-210 as a novel therapy for treatment of ischemic heart disease. Circulation 2010; 122 (11 Suppl): S124-31.
17. Besnier M, Gasparino S, Vono R, et al. miR-210 enhances the therapeutic potential of bone-marrow-derived circulating pro-angiogenic cells in the setting of limb ischemia. Mol Ther 2018; 26: 1694-705.
18. Zhu W, Sun L, Zhao P, et al. Macrophage migration inhibitory factor facilitates the therapeutic efficacy of mesenchymal stem cells derived exosomes in acute myocardial infarction through upregulating miR-133a-3p. J Nanobiotechnology 2021; 19: 61.
19. Li W, Liu Y, Zhang P, et al. Tissue-engineered bone immobilized with human adipose stem cells-derived exosomes promotes bone regeneration. ACS Appl Mater Interfaces 2018; 10: 5240-54.

20. Li Z, Guo X, Wu S. Epigenetic silencing of KLF2 by long non-coding RNA SNHG1 inhibits periodontal ligament stem cell osteogenesis differentiation. Stem Cell Res Ther 2020; 11: 435.
21. Liao Z, Luo R, Li G, et al. Exosomes from mesenchymal stem cells modulate endoplasmic reticulum stress to protect against nucleus pulposus cell death and ameliorate intervertebral disc degeneration in vivo. Theranostics 2019; 9: 4084-100.
22. Kumar B, Garcia M, Weng L, et al. Acute myeloid leukemia transforms the bone marrow niche into a leukemia-permissive microenvironment through exosome secretion. Leukemia 2018; 32: 575-87.
23. Yu J, Zhang L, Zhang H. Atorvastatin combined with routine therapy on HIF-1, VEGF concentration and cardiac function in rats with acute myocardial infarction. Exp Ther Med 2020; 19: 2053-8.
24. Hu JL, Wang W, Lan XL, et al. CAFs secreted exosomes promote metastasis and chemotherapy resistance by enhancing cell stemness and epithelial-mesenchymal transition in colorectal cancer. Mol Cancer 2019; 18: 91.
25. Monguio-Tortajada M, Prat-Vidal C, Moron-Font M, et al. Local administration of porcine immunomodulatory, chemotactic and angiogenic extracellular vesicles using engineered cardiac scaffolds for myocardial infarction. Bioact Mater 2021; 6: 3314-27.
26. Liang ZG, Yao H, Xie RS, et al. MicroRNA-20b-5p promotes ventricular remodeling by targeting the TGF-beta/Smad signaling pathway in a rat model of ischemia-reperfusion injury. Int J Mol Med 2018; 42: 975-87.
27. Chen K, Yan M, Li Y, et al. Intermedin1-53 enhances angiogenesis and attenuates adverse remodeling following myocardial infarction by activating AMP-activated protein kinase. Mol Med Rep 2017; 15: 1497-506.
28. Zhuang Y, Cheng M, Li M, et al. Small extracellular vesicles derived from hypoxic mesenchymal stem cells promote vascularized bone regeneration through the miR-210-3p/EFNA3/PI3K pathway. Acta Biomater 2022; 150: 413-26.
29. Shao H, Im H, Castro CM, et al. New technologies for analysis of extracellular vesicles. Chem Rev 2018; 118: 1917-50.
30. Kennedy TL, Russell AJ, Riley P. Experimental limitations of extracellular vesicle-based therapies for the treatment of myocardial infarction. Trends Cardiovasc Med 2021; 31: 405-15.
31. Todorova D, Simoncini S, Lacroix R, et al. Extracellular vesicles in angiogenesis. Circ Res 2017; 120: 1658-73.
32. Chistiakov DA, Orekhov AN, Bobryshev YV. Cardiac extracellular vesicles in normal and infarcted heart. Int J Mol Sci 2016; 17: 63.
33. Wang N, Chen C, Yang D, et al. Mesenchymal stem cells-derived extracellular vesicles, via miR-210, improve infarcted cardiac function by promotion of angiogenesis. Biochim Biophys Acta Mol Basis Dis 2017; 1863: 2085-92.
34. Yan H, Ma F, Zhang Y, et al. miRNAs as biomarkers for diagnosis of heart failure: a systematic review and meta-analysis. Medicine 2017; 96: e6825.
35. Kir D, Schnettler E, Modi S, Ramakrishnan S. Regulation of angiogenesis by microRNAs in cardiovascular diseases. Angiogenesis 2018; 21: 699-710.
36. Schneider S, Silvello D, Martinelli NC, et al. Plasma levels of microRNA-21, -126 and -423-5p alter during clinical improvement and are associated with the prognosis of acute heart failure. Mol Med Rep 2018; 17: 4736-46.
37. Nabialek E, Wańha W, Kula D, et al. Circulating microRNAs (miR-423-5p, miR-208a and miR-1) in acute myocardial infarction and stable coronary heart disease. Minerva Cardioangiol 2013; 61: 627-37.
38. Safran M, Masoud R, Sultan M, et al. Extracellular vesicular transmission of miR-423-5p from HepG2 cells inhibits the differentiation of hepatic stellate cells. Cells 2022; 11: 1715.
39. Qingju L, Xu Y, Kaiqi L, et al. Small extracellular vesicles containing miR-486-5p promote angiogenesis after myocardial infarction in mice and nonhuman primates. Sci Transl Med 2021; 13: eabb0202.